Spectrochimica Acta Part B 69 (2012) 25–31

Contents lists available at SciVerse ScienceDirect

Spectrochimica Acta Part B

journal homepage: www.elsevier.com/locate/sab

Metal argide (MAr^+) ions are lost during ion extraction in laser ablation-inductively coupled plasma-mass spectrometry

Travis M. Witte [1], R.S. Houk *

Ames Laboratory U. S. Department of Energy, Department of Chemistry, Iowa State University, Ames IA 50011 USA

ARTICLE INFO

Article history:
Received 29 October 2011
Accepted 28 February 2012
Available online 7 March 2012

Keywords:
ICP-MS
Laser ablation
Polyatomic ions
Metal argide ions
MAr^+ ions

ABSTRACT

The abundance of metal argide (MAr^+) ions during laser ablation-inductively coupled plasma-mass spectrometry (LA-ICP-MS) is measured during ablation of pure samples of transition metals. As expected, the relative abundance of MAr^+ ions to M^+ ions for various elements increases as the dissociation energy (D_0) of the ion increases. Gas kinetic temperatures (T_{gas}) are determined from the calculated MAr^+/M^+ ratios and are used to indicate the origins of MAr^+ ions. The determined T_{gas} values are very high, 8000 K to ≥20,000 K, which indicate that MAr^+ ions are much less abundant in the mass spectrum than expected based upon plasma conditions. Collision-induced dissociation (CID) during the ion extraction process is suggested to be responsible for removal of MAr^+ ions. Factors responsible for these collisions are discussed.

1. Introduction

Inductively coupled plasma mass spectrometry (ICP-MS) is one of the most sensitive techniques for atomic analysis, owing to the efficiency and robustness of the ICP as an atomic ion source [1,2]. The gas composition of the plasma is a significant factor in determining the ionization efficiency of the ICP. While a number of gases have been utilized to generate the ICP, including N_2 [3,4], O_2 [5], He [6,7], Ne [8], and air [3,9], argon remains the gas of choice for plasma generation in ICP-MS. Argon offers several advantages for ICP operation. Compared to some alternative gases, the low cost of Ar better suits it for the high gas consumption needed for long-term operation of the plasma. The ionization energy of Ar (15.76 eV) and the excitation energy of the first excited state (11.55 eV) are sufficiently high to achieve greater than 90% ionization of most elements but low enough that formation of doubly charged analyte ions is minor [10]. As an inert gas Ar is chemically unreactive with analyte species in the plasma, which minimizes the formation of unwanted molecular ions during atomic analysis.

Molecular Ar species are not absent entirely, however. Given the high number density of Ar in the ICP, if even a small percentage of Ar atoms form molecular ions with other species in the plasma, the resulting Ar-based polyatomic ion interferences can significantly impact the mass spectrum. Diatomic ions such as Ar_2^+, ArH^+ and ArO^+, which incorporate the major background ions Ar^+, H^+ and O^+, are the most abundant of these interferences [1]. These ions are endemic to ICP-MS analyses, particularly those in which the sample is introduced as a solution. Accordingly, studies have been undertaken of this variety of Ar polyatomic ion to better understand the fundamental processes in the ICP related to their abundance in the mass spectrum [11–13].

Interferences arising from the formation of Ar adducts with M^+ ions from elements in the sample matrix are less prominent but may still lead to significant complications. Unlike the polyatomic ions formed by the combination of Ar and background species, where only the same handful of m/z values must be monitored for interference, an Ar-based interference is possible at every mass equal to that of the analyte and the major isotope of Ar combined. In certain m/z regions these MAr^+ ions cannot be readily resolved from so-called "isobaric" atomic analyte ions with high-resolution magnetic sector instruments. Samples like steel alloys could contain several such abundant matrix elements. Foreknowledge of sample composition and chemical separations can assist in surmounting this obstacle but may complicate the analysis or be impracticable in some situations.

One such situation is encountered for solid samples where spatial integrity needs to be preserved, whether to gain additional information during the analysis or to minimize the destruction of a valuable sample. Laser ablation (LA)-ICP-MS can readily analyze these samples, with the concession that all species present in the sample, including those that may form polyatomic interferences, will be introduced into the ICP-MS. Guillong et al. describe a specific case where these MAr^+ ions complicate analysis, the determination of Platinum Group Elements (PGEs) in ore samples [14]. The base metals that occur alongside PGEs in these samples can form metal argide ions (MAr^+) that occur at almost the same m/z values as the M^+ ions from the low-abundance PGEs.

* Corresponding author. Tel.: +1 515 294 9462; fax: +1 515 294 0105.
E-mail address: rshouk@iastate.edu (R.S. Houk).
[1] Present address: Department of Chemistry, University of Kansas, Lawrence KS 66045-4401 USA.

0584-8547/$ – see front matter © 2012 Elsevier B.V. All rights reserved.
doi:10.1016/j.sab.2012.02.008

Studies to better understand and address MAr^+ ions in ICP-MS analyses, for either solution nebulization or LA, have been undertaken by only a few investigators [15,16]. Becker et al. compared the abundance of MAr^+ ions in solution nebulization ICP-MS, LA-ICP-MS and glow discharge (GD)-MS and investigated the periodic nature of their abundances [17]. Guillong et al. described the effect of the mass spectrometer interface design in commercial quadrupole instruments on MAr^+ ion abundance [14].

The present work seeks to further build upon the knowledge about MAr^+ ions presented in these investigations. By comparing theoretical calculations of the MAr^+/M^+ ion ratio at various conditions with a MAr^+/M^+ ratio measured from empirical ion signals, the conditions responsible for the observed abundance of MAr^+ ions can be determined. Potentially, information on the origin of these ions could be utilized to develop broad strategies needed for their reduction.

2. Theory

2.1. Determination of polyatomic ion origin

Prior investigations from our group have developed a general method to describe the origins of polyatomic ions in ICP-MS [11,13,18,19]. The basis of this method is a proposed dissociation reaction for the polyatomic species, MAr^+.

$$MAr^+ \rightleftharpoons M^+ Ar \quad \Delta H = D_0\left(MAr^+\right) \tag{1}$$

Experimental data are collected and used to evaluate a dissociation expression for the proposed reaction.

$$K_d = \left(\frac{n_{M^+}}{n_{MAr^+}}\right) n_{Ar} \tag{2}$$

In this expression, the ratio between the number densities (n) for M^+ and MAr^+ is assumed to be proportional to the ratio between the measured signals of the ions M^+ and MAr^+. Use of this measured signal ratio removes the need to ascertain the absolute number densities of each ion. An estimate of the number density of the neutral species (n_{Ar}) is made from known plasma conditions.

An alternative form of the same dissociation expression can be written in relation to the partition functions (Z) of each species, using the available spectroscopic constants (Table 1) [20–31].

$$K_d = \frac{Z_{Ar} Z_{M^+}}{Z_{MAr^+}} e^{-D_0/kT} \tag{3}$$

Table 1
Dissociation energies and spectroscopic data for first-row transition metal argide (MAr^+) ions. Both theoretical and experimental values are listed where available. The D_0 values actually used are indicated with asterisks.

		D_0 (eV)	ω (cm^{-1})	B (cm^{-1})	g	Term symbol	Refs.
$TiAr^+$	Theo	0.31*	163	0.110	8	$^4\Phi$	[20]
VAr^+	Theo	0.291	143	0.103	5	$^5\Sigma$	[21,22]
	Exp	0.369*		0.108			[22]
$CrAr^+$	Theo	0.239	111	0.085	6	$^6\Sigma$	[20]
	Exp	0.29*					[23]
$MnAr^+$	Theo	0.149*	93	0.090	7	$^7\Sigma$	[24]
$FeAr^+$	Theo	0.493	198	0.116	12	$^6\Delta$	[25,26]
	Exp	0.11*	98	0.092			[25]
$CoAr^+$	Theo	0.533	199	0.123	6	$^3\Delta$	[27,26]
	Exp	0.51*	265	0.124			[27,28]
$NiAr^+$	Theo	0.52	195	0.123	2	$^2\Sigma$	[24,26]
	Exp	0.55*	235	0.165			[29]
$CuAr^+$	Theo	0.53*	197	0.119	1	$^1\Sigma$	[24,26]
$ZnAr^+$	Theo	0.322	132	0.101	2	$^2\Sigma$	[26,30,31]
	Exp	0.25*					[30]

In the expanded form of this expression (not shown), the electronic partition function is assumed to be equal to the statistical weight (g) of the ground state of the ion MAr^+. When the term symbol of the ground state is sigma, g = the multiplicity of ion. For all other term symbols, g = 2 * (multiplicity of the ground electronic state of MAr^+) [32,33]. Calculation of the electronic partition function for M^+ utilizes a polynomial equation valid from 1500 to 12,000 K for each element [34,35]. Use of these equations at greater temperatures represents the best approximation available and is necessary for the very high gas kinetic temperature (T_{gas}) values encountered in the present study. Both the neutral Ar number density and the partition functions depend on the gas kinetic temperature and thus are calculated across a range of T_{gas} values. In this study, the range of T_{gas} values extends well beyond the upper limit cited for the atomic partition functions.

A T_{gas} value is determined for the reaction by comparing the measured dissociation constant (K_d) from Eq. (2) and theoretical dissociation constant from Eq. (3) across the likely range of reasonable T_{gas} values. The value at which the measured and theoretical K_d values best agree is assigned as the T_{gas} representative of the conditions responsible for the abundance of polyatomic ions in the spectrum.

Based on these T_{gas} values, there are three possible assignments that can be made for the origin of the polyatomic ion.

(1) If T_{gas} values are between ~5000 to 6000 K, the polyatomic ion abundance in the spectrum is consistent with that expected in the plasma. Post-plasma effects do not alter the polyatomic ion abundance.
(2) If T_{gas} is greater than ~6000 K, some process(es) during ion extraction removes the polyatomic ion, leaving it less abundant in the spectrum than expected based on plasma conditions alone.
(3) If T_{gas} is below ~5000 K, some process(es) during extraction creates additional polyatomic ions, causing it to be more abundant in the spectrum than expected based on plasma conditions alone.

3. Experimental

3.1. Instrumentation

LA-ICP-MS experiments were conducted using an LSX-500 (CETAC Technologies, Inc., Omaha, NE) connected to an XSeries 2 (Thermo Fisher Scientific, Inc., Bremen, Germany). The LSX-500 is a 266 nm Nd:YAG system with a laser pulse width of 5 ns and maximum energy output of 9 mJ. Beam characteristics, including laser energy, repetition rate and spot size are selected through software. The XSeries 2 ICP-MS was operated with a grounded guard electrode to minimize the secondary discharge and kinetic energy spread in the ions. This device is a quadrupole, unlike the magnetic sector instrument utilized in most of our previous papers on polyatomic ions [36]. A collision cell is available in this instrument but was operated with no added collision gas. This ensured that polyatomic ion abundances were influenced solely by conditions in the plasma and extraction interface.

Although He is commonly used as carrier gas during LA, all gas flows were Ar in the present paper. This simplifies calculation of $n_{Ar} = P/RT_{gas}$ in Eq. (2). Most gas flows were regulated with the internal mass flow controllers of the XSeries 2. An external Ar mass flow controller was used to control the aerosol gas flow for laser ablation. The instrument was tuned using atomic ions from nebulized solutions to maximize signal and still provide reasonable stability. The torch inlet was then connected to the laser system for final adjustment before data collection. Settings for both the LSX-500 and XSeries 2 are summarized in Table 2.

Table 2
LA-ICP-MS operating parameters.

ICP-MS instrument	Thermo XSeries 2
Torch	Shielded (grounded Pt guard electrode)
Interface configuration	Xt (Ni sampler and skimmer cones)
RF power	1400 W
Outer gas	13 L min^{-1}
Auxiliary gas	0.7 L min^{-1}
Aerosol gas	1.0 L min^{-1}
Detector mode	Dual (analog and pulse counting) Cross-calibrated
Laser system	LSX-500 Nd:YAG 266 nm
Energy	8.65 mJ
Spot size	150 μm
Repetition rate	10 Hz
Ablation mode	Raster (100 μm s^{-1})

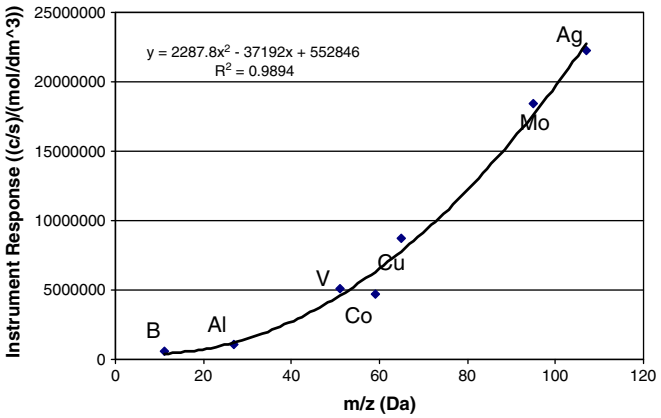

Fig. 1. Instrument response plot from ablation of NIST 1263a steel for mass bias corrections.

3.2. Sample materials

Single metal samples (Materials Preparation Center, Ames Laboratory, U.S. Department of Energy, Ames, IA) were obtained for each of nine first-row transition metals (Ti, V, Cr, Mn, Fe, Co, Ni, Cu, Zn). Since the MAr^+ ions occur at low abundance, they could be mistaken for M^+ ions from impurity elements, which is why samples of single metals were chosen and ablated individually. Various isotopes corresponding to heavy metal impurities were monitored, which confirmed that only MAr^+ ions were detected at the masses of interest, not M^+ ions from elemental impurities. NIST 1263a Cr–V Modified Steel was ablated to collect multielement data for construction of a mass bias plot.

3.3. Estimation of neutral density (n_{Ar})

It is necessary to estimate the number density of the neutral species in the proposed dissociation reaction to calculate the measured dissociation constant. For the MAr^+ ions examined in this study, that requires estimation of the number density of neutral Ar. The number density of the major components in the plasma can be estimated using the ideal gas law.

$$n_{total} = n_{Ar} + n_H + n_O = P/RT_{gas} \quad (4)$$

In LA-ICP-MS experiments, n_H and n_O (~4×10^{15} and 2×10^{15} cm^{-3}, respectively) are assumed to negligible relative to n_{Ar} (~1×10^{18} cm^{-3} at P = 1 atm and T_{gas}~6000 K), especially when ablating metals.

3.4. Mass bias corrections

The preferential transmission and detection of heavier ions relative to lighter ions, known as mass bias, is an issue in ICP-MS. Corrections for this behavior are necessary for analyses involving the measurement of accurate isotope ratios, especially when the mass difference between isotope masses is large. The MAr^+ ions in this study present an extreme case, with M^+ ions 40 Da lighter than their corresponding MAr^+ ion. The effect of these corrections on the isotope ratios studied for this work is discussed in detail elsewhere in this paper.

A multielement response curve [12,37] was used in this study in cases where mass bias corrections were employed. For this purpose, NIST 1263a, a steel standard, was chosen as a multielement sample that should ablate like the single-element metals. This standard contained elements across the mass range of interest in this work (up to $m/z = 107$). After correcting for isotopic abundance and ionization efficiency ($T_{ion} = 7500$ K, $n_e = 1\times10^{15} cm^{-3}$), a polynomial was fit to the collected data, as shown in Fig. 1. All multielement data were collected after analysis of the pure metal samples so that no residual atomic ions from ablation of the standard were available to interfere with measurement of MAr^+ ion abundances.

4. Results and discussion

4.1. Measured MAr^+/M^+ signal ratios and T_{gas} values

The MAr^+/M^+ (M = Ti, V, Cr, Mn, Fe, Co, Ni, Cu, Zn) signal ratios were measured for nine first-row transition metals and are presented both with and without mass bias corrections in Table 3. These signal ratios in the table are multiplied by 10^6 and are thus shown in ppm for convenient comparison. They are comparable to those measured by Becker et al. [17] and by Guillong et al. [14] for several of the same MAr^+ ions. The ratios found by Guillong et al. [14], included for comparison in Table 3, provide suitable points of reference for the MAr^+/M^+ ratios in this study, as they were collected on the same model of ICP-MS (XSeries 2). Their measured ratios are higher than ours by factors of 5 to 8. This disparity may be partially attributed to several factors. Different mass bias correction methods and cones of different geometries (even for the same basic Thermo *X*2 instrument) were used in the two studies. Guillong et al. used He carrier gas, while we used Ar only. Despite these differences, the T_{gas} values calculated from the ratios published by Guillong et al. also correspond to high T_{gas} values, which indicate a fate similar to that found in this work for MAr^+ ions, as discussed below.

The low abundance of each MAr^+ ion relative to the corresponding M^+ ion (1 to 10 ppm, ~10^{-6} to 10^{-5}) is expected for this type of polyatomic ion. Even under plasma conditions, the formation of argon-based diatomic ions with metals is not favored energetically. Experimentally and theoretically determined dissociation energies for MAr^+ ions incorporating transition metals (Table 1) [20–31] are no higher than 0.55 eV, which illustrates the weakly bound nature of these ions. Despite this the absolute abundance of MAr^+ interferences can still have a significant impact on trace element detection when M represents a matrix element.

4.2. Trends in MAr^+ ratios and D_0 values

A general trend of decreasing dissociation energies from Ti to Fe, followed by a marked increase centered on Ni, has been found for transition metal-based MAr^+ ions. Because these values are collected from several sources, discrepancies in the degree of change in D_0 values between species, and even exceptions to the trend (e.g., VAr^+), are found. Nonetheless, a broad correlation is observed between increasing MAr^+/M^+ ratios and increasing dissociation energies across the period of the first-row transition metals. Both the upper and lower bounds of MAr^+/M^+ ratios are established by the

Table 3
MAr^+/M^+ signal ratios (in ppm) and T_{gas} values for first-row transition metals.

	$FeAr^+$		$MnAr^+$		$CrAr^+$		$ZnAr^+$		$TiAr^+$	
Mass bias?	No	Yes	N	Y	N	Y	N	Y	N	Y
This study										
MAr^+/M^+	0.538	0.168	0.607	0.186	3.19	0.93	7.88	2.78	8.13	2.19
T_{gas} (K)	73,700	112,000	141,000	227,000	30,800	47,100	87,200	130,000	15,300	34,500
Guillong et al.										
MAr^+/M^+ [14]								18.0		
T_{gas} (K)								60300		

	VAr^+		$CoAr^+$		$CuAr^+$		$NiAr^+$	
Mass bias	N	Y	N	Y	N	Y	N	Y
This study								
MAr^+/M^+	1.35	0.385	4.67	1.53	9.18	3.06	12.5	4.04
T_{gas} (K)	32,200	62,000	13,700	18,400	17,100	22,400	8290	14,300
Guillong et al.								
MAr^+/M^+ [14]				13.0		15.0		20.0
T_{gas} (K)				9290		15,100		6740

most weakly ($FeAr^+$) and strongly ($NiAr^+$) bound ions, based on experimentally determined D_0 values.

Differences in the dissociation energies among MAr^+ ions may be influenced by both the electronegativity of the transition metal and electron configuration of the metal ion. It has been suggested that a more covalent-type interaction occurs between the metal ion and argon neutral for metals with higher electronegativities [17]. While this is a very weak covalent interaction for all transition metals with Ar, it would account for the higher MAr^+/M^+ ion ratios calculated for metals toward the right end of the period in the periodic table where the greatest electronegativities are found. Indeed the most electronegative of the metals studied, Ni (Pauling electronegativity = 1.8), shows the highest relative abundance of MAr^+ ions.

However, electronegativity patterns alone cannot fully account for the variation in the binding strength of the MAr^+ ions. If this trend were the sole controlling factor, the D_0 values for $FeAr^+$ (0.11 eV) and $CoAr^+$ (0.51 eV) should be similar due to identical electronegativity values (Pauling electronegativity = 1.7 for both), but they are quite different. The MAr^+/M^+ signal ratios measured for these species bear out the difference in binding strength, with the $CoAr^+/Co^+$ ratio approximately an order of magnitude greater than the $FeAr^+/Fe^+$ ratio. The cause of the weaker interaction between the Fe and Ar atoms, as compared to Co and Ar atoms, is likely related to the electron configuration of the metal ion.

Given the low ionization energy of most of the transition metals (6.7 to 7.9 eV, 9.29 eV for Zn) against that of argon (15.76 eV), it is expected that the formation of MAr^+ ions results from the interaction of an M^+ ion with neutral argon. Thus one of the factors in the reaction is the electronic state of the M^+ ion. The valence electron configuration of most first-row transition metals (Table 4) [38–40] includes only electrons in the 3d orbitals. Theoretical modeling has established that the absence of electrons in the 4s subshell reduces repulsion between metal ions and argon, enhancing the bond strength in the MAr^+ ion [20,24].

Those transition metal ions with 4s electrons (Mn^+, Fe^+) form much weaker diatomic ions with argon than nearby elements with empty 4s subshells. Both $MnAr^+$ and $FeAr^+$ were less abundant relative to their respective M^+ ions than the other MAr^+ ions measured. $TiAr^+$ appears to be an exception to this rule; the $TiAr^+$ cation has a more complex ground state electron configuration. Though the lowest energy and preferred configuration places an electron in the 4s subshell, $TiAr^+$ has a low lying electronic state with no electrons in the 4s subshell [20]. This state likely contributes to the population of Ti^+ ions in the ICP, forming a more stable diatomic ion with argon than would be otherwise expected from the lowest energy configuration alone.

Table 4
Valence electron configuration of first-row transition metal cations.

Ion	Ti^+	V^+	Cr^+	Mn^+	Fe^+	Co^+	Ni^+	Cu^+	Zn^+
Valence Configuration	$3d^24s^1$ ($3d^3$)	$3d^4$	$3d^5$	$3d^54s^1$	$3d^64s^1$	$3d^8$	$3d^9$	$3d^{10}$	$3d^{10}4s^1$
Refs.	[20,38]	[38]	[38]	[39]	[40]	[40]	[40]	[39]	[39]

4.3. Significance of very high measured T_{gas} values; effects of fundamental data and mass bias corrections

T_{gas} values (Table 3) were determined for each MAr^+ ion where all necessary spectroscopic values (Table 1) were available. Very high T_{gas} values that are greatly different for the various ions are found for the MAr^+ ions chosen. Even the lowest value (~8000 K for $NiAr^+$) is clearly above the typical T_{gas} range of the ICP (5000 to 6000 K). These observations indicate a) these polyatomic ions are much *less* abundant in the mass spectrum relative to the metal atomic ion than would be predicted based upon plasma conditions alone, and b) the lack of a uniform T_{gas} value shows their relative abundances to be far out of thermal equilibrium. Thus, some process(es) during ion extraction greatly *reduces* the abundance of MAr^+ relative to M^+.

Errors in the fundamental data are a possible cause for faulty T_{gas} values. The value for D_0 is particularly important [13]. The measured T_{gas} values are too large, so the D_0 values would all have to be too small to account for the observed lack of MAr^+ ions. Use of any of the alternative D_0 values listed in Table 1 does not affect the basic diagnosis that the MAr^+ ions are observed at abundances much less than expected from ICP conditions.

The MAr^+/M^+ ratios discussed have been presented without the mass bias corrections typically applied to isotope ratios calculated from ICP-MS spectral data. The basis for such corrections rests in constructing a plot of instrument response over a range of mass-to-charge values covering the isotope masses of interest. Instrument response is calculated by adjusting the measured atomic ion signal for isotopic abundance, ionization efficiency in the ICP and concentration in the multielement standard used. From this the preferential transmission of heavier isotopes, often attributed chiefly to space charge effects that cause greater repulsive losses of lighter ions [41], can be corrected in isotope ratio calculations. This approach should be generally valid when correcting atomic ion ratios, whose behavior is appropriately represented by the atomic ions used to create the instrument response curve.

For lack of something better, this same approach to mass bias corrections has been used previously for polyatomic ions. This approximation is probably reasonable when the T_{gas} measurements indicate the polyatomic ions originate from the plasma itself. It is not clear that it is valid when the measured signal ratios and T_{gas} values expressly show that the polyatomic ions are attenuated during ion extraction. Additional factors beyond space charge effects could alter the observed ion abundances. In particular, the instrument response curve from atomic ions cannot account for the dissociation of MAr^+ ions during extraction. For example, the instrument response curve created for this study (Fig. 1) would predict that the polyatomic ion $^{64}Zn^{40}Ar^+$ would be transmitted at 3x the level of the lighter $^{64}Zn^+$ atomic ion, based on the loss of ions at $m/z = 64$ relative to those at $m/z = 104$. The mass difference between a MAr^+ ion and its M^+ analogue is 40 Da, the highest value for any abundant polyatomic ion and thus subject to the largest numerical mass bias correction. If, however, MAr^+ ions are dissociated to a very high degree during extraction, it is hard to say that the MAr^+ ions are still transmitted 3× more efficiently than the corresponding M^+ ions.

Uncertainty as to the proper exercise of mass bias corrections would seem to be a significant hurdle in the use of MAr^+/M^+ ion ratios for the determination of T_{gas} and polyatomic ion origins. Given the large relative mass difference between the ions, application of mass bias corrections to MAr^+/M^+ ion ratios greatly influences the measured ion signal ratio (Table 3). The measured ratios are reduced by a factor of ~3 with these corrections, which makes the measured T_{gas} values higher than 6000 K *by even greater amounts*. As was the case with D_0 values, doubt about the validity of mass bias corrections again does not affect the assignment of ion origins, which is the primary goal of the work. The determined T_{gas} values still indicate extensive removal of MAr^+ ions during ion extraction. Therefore, questions about the mass bias model used in this study does not alter the conclusion that processes during ion extraction reduce the abundance of MAr^+ ions.

4.4. Suggested causes of low MAr^+ abundances: collision-induced dissociation?

For weakly bound MAr^+ ions, collisions in the regions after the sampler and/or skimmer could readily result in the fragmentation of the polyatomic ion. Such a mechanism is in line with the proposal by Guillong et al. that flow restrictions through the extraction lens behind the skimmer cone promote collisions that dissociate MAr^+ ions [14]. We also provide T_{gas} values derived from their measurements of MAr^+/M^+ ions with an XSeries 2, the same device used in this study, in Table 3. Even with relative MAr^+ abundances greater than those found in this study, all T_{gas} values are still much higher than 6000 K, again indicating extensive removal of these ions during extraction.

Consider again the low MAr^+/M^+ signal ratios found, either by Guillong or in the present work. For the MAr^+ ions to be present in the mass spectrum at levels expected based on plasma conditions, the relative abundance of MAr^+ ions would need to be higher by 1 to 3 orders of magnitude than those observed experimentally (Table 5). If it is assumed that observed MAr^+ ion signal represents the fraction that survive after ion extraction from the plasma, up to 99% of transition metal MAr^+ ions are lost during ion extraction.

These considerations clearly indicate that processes occurring during ion extraction actually remove most of the MAr^+ ions. This observation is somewhat surprising given that fundamental studies of these ions use supersonic expansions for the reverse objective—to make them. The early predictions of Douglas [42] are borne out once again, that the high temperature of the ICP actually suppresses the abundances of weakly bound polyatomic ions, compared to much cooler gas sources used to make them deliberately for fundamental studies.

Table 5
Comparison of measured MAr^+/M^+ signal ratios and ratios expected from plasma conditions ($T_{gas} = 6000$ K) (all ratios in ppm).

	D_0 (eV)	Measured MAr^+/M^+ signal ratio	MAr^+/M^+ signal ratio at 6000 K	% of MAr^+ removed
$FeAr^+$	0.11	0.538	58.1	99.1
$MnAr^+$	0.149	0.607	295	99.8
$ZnAr^+$	0.25	7.88	274	97.1
$CrAr^+$	0.29	3.19	314	99.0
$TiAr^+$	0.31	8.13	32.7	75.1
VAr^+	0.369	1.35	31.2	95.7
$CoAr^+$	0.51	4.67	31.5	85.2
$CuAr^+$	0.53	9.18	229	96.0
$NiAr^+$	0.55	12.5	26.3	52.5

We suggest that the MAr^+ ions may be dissociated by the existence of a small potential between the plasma and the mass spectrometer interface. In this experiment, a grounded metal shield is used between the load coil and the outside of the torch. The free electrons in the metal shield prevent the potential gradient on the load coil from coupling capacitively to the plasma [43–45]. However, the shield does not cover the entire outside of the torch; a small gap (~2.2 mm wide) is left to prevent buildup of circulating currents that would otherwise melt the shield [43]. Thus, a small potential may be induced in the plasma from the voltage gradient down the load coil propagated through this gap.

Such a potential can readily penetrate into the region between the sampler and skimmer, as shown by old Langmuir probe measurements [46]. As ions travel between the plasma and the sampler, or between the sampler and skimmer, they gain energy from the potential gradient and also collide with background Ar gas atoms. The situation is analogous to that encountered with a nozzle-skimmer extraction system in electrospray MS; the skimmer can be biased at a potential more negative than that of the nozzle to fragment the positive ions [47]. In the present work, a potential of only 2 volts would result in a center-of-mass collision energy of $2\,eV^*[m_{Ar}/(m_{Ar}+m_{MAr+})]$ ~0.8 eV, well above the dissociation energies of any of the MAr^+ ions ($m^+_{MAr} = 90$ to 100 Da, $D_0 = 0.1$ to 0.55 eV) examined in this study. Given the high T_{gas} values found for some other weakly bound polyatomic ions, especially ArO^+ ($D_0 = 0.312$ eV) [48], collisions and energy transfer induced by the plasma potential may actually remove other weakly bound polyatomic ion interferences and thus be desirable.

Douglas [42] suggests a similar CID effect behind the skimmer. In the present work, the skimmer is grounded, and there is a cylindrical extraction lens at ~−200 V just behind it. Thus, there is a potential gradient aft of the skimmer that could accelerate ions through the supersonic beam and cause them to dissociate. If most of the collisions occur near the skimmer tip, the potential there is only a small fraction of the voltage on the extraction lens, so only weakly bound ions like MAr^+ gain enough energy to dissociate in this region. Guillong et al. [14] suggest such CID occurs due to collisions that take place after the skimmer as the beam goes into the extraction lens. Farnsworth and co-workers [49–51] have found shock waves both just before and just after the skimmer tip for many brands of skimmer. Collisions in these shocks could also play a role in the loss processes noted for MAr^+ in the present paper.

5. Conclusion

Measured MAr^+/M^+ ion ratios from ablation of pure transition metals are similar to those determined experimentally by other investigators for these species in LA-ICP-MS. The measured ion ratios increase with the dissociation energy of each MAr^+ ion, with a few exceptions. Transition metal ions with one or more 4s electrons in the ground state configuration form the most weakly bound MAr^+

ions, as the $MnAr^+/Mn^+$ and $FeAr^+/Fe^+$ ratios illustrate. Contributions from an empty 4s subshell configuration to the ground state of Ti^+ stabilize the $TiAr^+$ ion, resulting in a larger MAr^+/M^+ ratio than for the $MnAr^+$ and $FeAr^+$ ions.

T_{gas} values much greater than 6000 K are found for all transition metal-based MAr^+ ions studied, indicating very extensive dissociation of the polyatomic ions during ion extraction. Examination of literature on supersonic beams leads to the expectation that collisions during extraction would cause formation of *more* MAr^+ ions than are present in the plasma; precisely the opposite effect is seen. Collisions during the extraction process actually *remove* most of the weakly bound MAr^+ ions relative to the level expected based on plasma conditions.

Several phenomena during the ion extraction process could be responsible for these collisions. Flow restrictions between the skimmer and extraction lens could increase the number of collisions as the ions are sampled from the plasma [14]. This effect could be studied by varying the geometry of both sampler and skimmer, as well as the spacing between them. There may exist a small plasma potential due to incomplete shielding of the ICP by the guard electrode. This small plasma potential may nonetheless be strong enough to bring about collisions of sufficient energy to dissociate MAr^+ ions during extraction process. The very high T_{gas} values consistently measured for ArO^+ [48] may also reflect CID in this manner.

Ion kinetic energy distributions could be studied to establish whether such a plasma potential exists for the shielded plasmas commonly used at present. The effect of various extraction lens voltages on relative ion abundances could clarify the possible role of CID behind the skimmer. Guillong et al. [14] did not find large differences in MAr^+ abundances as extraction lens voltage was changed. Our initial results (data not shown) agree with their observations, which argue that the dissociation reactions have occurred before the ions go very far behind the skimmer tip. Such information could prove valuable not only to understanding those processes related to polyatomic ion abundances but to general knowledge of ion extraction conditions in current ICP-MS instrumentation as well.

Acknowledgements

This research was supported by the U. S. Department of Energy, Office of Nuclear Nonproliferation (NA-22). The XSeries 2 ICP-MS was purchased with funds provided by the U. S. Department of Energy, Office of Nuclear Nonproliferation (NA-22) and the Office of Basic Energy Sciences. The authors thank Larry Jones and the Materials Preparation Center at the Ames Laboratory for providing the transition metal samples. The Ames Laboratory is operated for the U. S. Department of Energy by Iowa State University under Contract No. DE-AC02-07CH11358.

References

[1] R.S. Houk, V.A. Fassel, G.D. Flesch, H.J. Svec, A.L. Gray, C.E. Taylor, Inductively coupled argon plasma as an ion source for mass spectrometric determination of trace elements, Anal. Chem. 52 (1980) 2283–2289.
[2] K.E. Jarvis, A.L. Gray, R.S. Houk, Handbook of Inductively Coupled Plasma Mass Spectrometry, Chapman and Hall, New York, 1992.
[3] G.A. Meyer, R.M. Barnes, Analytical inductively coupled nitrogen and air plasmas, Spectrochim. Acta Part B 40 (1985) 893–905.
[4] H. Uchida, T. Ito, Inductively coupled nitrogen plasma mass spectrometry assisted by adding argon to the outer gas, J. Anal. At. Spectrom. 10 (1995) 843–848.
[5] P. Yang, R.M. Barnes, A low-power oxygen inductively coupled plasma for spectrochemical analysis—IV. Analytical features, Spectrochim. Acta Part B 45 (1990) 167–176.
[6] H. Hayashi, M. Hiraide, Low-pressure helium ICP-MS for trace analysis, Bunseki Kagaku 53 (2004) 793–804.
[7] T. Nagayasu, H. Hayashi, M. Hiraide, Laser ablation and low-pressure helium-ICP-MS for the analysis of alumina powder dispersed in glycerol, Anal. Sci. 21 (2005) 1411–1413.
[8] T. Manning, G. Bentley, B. Palmer, D. Hof, Generation of a low flow atmospheric pressure neon ICP, Spectrosc. Lett. 22 (1989) 341–344.
[9] G.A. Meyer, Determination of metals in xylene by inductively coupled air plasma emission spectrometry, Spectrochim. Acta Part B 42 (1987) 201–206.
[10] H. Niu, R.S. Houk, Fundamental aspects of ion extraction in inductively coupled plasma mass spectrometry, Spectrochim. Acta Part B 51 (1996) 779–815.
[11] R.S. Houk, N. Praphairaksit, Dissociation of polyatomic ions in inductively coupled plasma, Spectrochim. Acta Part B 56 (2001) 1069–1096.
[12] J.W. Ferguson, R.S. Houk, High resolution studies of the origins of polyatomic ions in inductively coupled plasma-mass spectrometry, Part I. Identification methods and effects of neutral gas density assumptions, extraction voltage, and cone material, Spectrochim. Acta Part B 61 (2006) 905–915.
[13] S.M. McIntyre, J.W. Ferguson, T.M. Witte, R.S. Houk, Measurement of gas kinetic temperatures for polyatomic ions in inductively coupled-plasma mass spectrometry: validation and refinements, Spectrochim. Acta Part B 66 (2011) 248–254.
[14] M. Guillong, L. Danyushevsky, M. Walle, M. Raveggi, The effect of quarupole ICPMS interface and ion lens design on argide formation. Implications for LA-ICPMS analysis of PGE's in geological samples, J. Anal. At. Spectrom. 26 (2011) 1401–1407.
[15] B. Hattendorf, D. Günther, M. Schönbächler, A. Halliday, Simultaneous ultratrace determination of zr and nb in chromium matrixes with ICP-dynamic reaction cell MS, Anal. Chem. 73 (2001) 5494–5498.
[16] M.-F. Zhou, J. Malpas, M. Sun, Y. Liu, X. Fu, A new method to correct Ni- and Cu-argide interference in the determination of the platinum-group elements, Ru, Rh, and Pd, by ICP-MS, Geochem. J. 35 (2001) 413–420.
[17] J.S. Becker, G. Seifert, A.I. Saprykin, H.-J. Dietze, Mass spectrometric and theoretical investigations into the formation of argon molecular ions in plasma mass spectrometry, J. Anal. At. Spectrom. 11 (1996) 643–648.
[18] H.P. Longerich, Mass spectrometric determination of the temperature of an argon inductively coupled plasma from the formation of the singly charged monoxide rare earths and their known dissociation energies, J. Anal. Atom. Spectrom. 4 (1989) 491–497.
[19] E.H. Evans, L. Ebdon, L. Rowley, Comparative study of the determination of equilibrium dissociation temperature in inductively coupled plasma-mass spectrometry, Spectrochim. Acta Part B 57 (2002) 741–754.
[20] H. Partridge, C.W. Bauschlicher Jr., Theoretical study of the low-lying states of $TiHe^+$, $TiNe^+$, $TiAr^+$, VAr^+, $CrHe^+$, $CrAr^+$, $FeHe^+$, $FeAr^+$, $CoHe^+$, and $CoAr^+$, J. Chem. Phys. 98 (1994) 2301–2306.
[21] C.W. Bauschlicher Jr., H. Partridge, S.R. Langhoff, Theoretical study of metal noble-gas positive ions, J. Chem. Phys. 91 (1989) 4733–4737.
[22] T. Hayes, D. Bellert, T. Buthelezi, P.J. Brucat, The bond length of VAr^+, Chem. Phys. Lett. 287 (1998) 22–28.
[23] D.E. Lessen, R.L. Asher, P.J. Brucat, Spectroscopically determined binding energies of $CrAr^+$ and $Cr(N_2)^+$, Chem. Phys. Lett. 177 (1991) 380–382.
[24] B.L. Hammond, W.A. Lester Jr., M. Braga, C.A. Taft, Theoretical study of the interaction of ionized transition metals (Cr, Mn, Fe, Co, Ni, Cu) with argon, Phys. Rev. A 41 (1990) 10447–10452.
[25] B.L. Tjelta, D. Walter, P.B. Armentrout, Determination of weak Fe^+–L bond energies (L = Ar, Kr, Xe, N_2, and CO_2) by ligand exchange reactions and collision-induced dissociation, Int. J. Mass Spectrom. 204 (2001) 7–21.
[26] T. Bastug, W.-D. Sepp, B. Fricke, E. Johnson, C.M. Barshick, All-electron relativistic Dirac–Fock–Slater self-consistent-field calculations of the singly charged diatomic transition-metal- (Fe, Co, Ni, Cu, Zn) argon molecules, Phys. Rev. A 52 (1995) 2734–2736.
[27] R.L. Asher, D. Bellert, T. Buthelezi, P.J. Brucat, The ground state of $CoAr^+$, Chem. Phys. Lett. 227 (1994) 277–282.
[28] D. Lessen, P.J. Brucat, Resonant photodissociation of $CoAr^+$ and $CoKr^+$: analysis of vibrational structure, J. Chem. Phys. 90 (1989) 6296–6305.
[29] D. Lessen, P.J. Brucat, On the nature of $NiAr^+$, Chem. Phys. Lett. 152 (1988) 473–476.
[30] A.W.K. Leung, D. Bellert, R.R. Julian, W.H. Breckenridge, Resonant two-color photoionization threshold measurements of the Zn^+ (4s) Ar bond strength: model-potential analysis of M^+ (ns) Ar interactions, J. Chem. Phys. 110 (1999) 6298–6305.
[31] C.M. Barshick, D.H. Smith, E. Johnson, F.L. King, T. Bastug, B. Fricke, Periodic nature of metal-noble gas adduct ions in glow discharge mass spectrometry, Appl. Spectrosc. 49 (1995) 885–889.
[32] R.E. Sonntag, G.J. Van Wylen, Fundamentals of Statistical Thermodynamics, John Wiley and Sons, Inc., New York, 1966.
[33] N.M. Laurendeau, Statistical Thermodynamics: Fundamentals and Applications, Chapter 9, Cambridge University Press, Cambridge, 2005.
[34] L. De Galan, R. Smith, J.D. Winefordner, The electronic partition functions of atoms and ions between 1500 K and 7000 K, Spectrochim. Acta Part B 23 (1968) 521–525.
[35] S. Tamaki, T. Kuroda, The electronic partition functions of atoms and ions between 7000 K and 12 000 K, Spectrochim. Acta Part B 42 (1987) 1105–1111.
[36] T.M. Witte, Laser ablation-inductively coupled plasma-mass spectrometry: examinations of the origins of polyatomic ions and advances in the sampling of particulates, Thesis (Ph. D.)Iowa State University, 2011.
[37] C.P. Ingle, B.L. Sharp, M.S.A. Horstwood, R.R. Parrish, D.J. Lewis, Instrument response functions, mass bias, and matrix effects in isotope ratio measurements and semi-quantitative analysis by single and multi-collectore ICP-MS, J. Anal. Atom. Spectrom. 18 (2003) 219–229.
[38] B.L. Kickel, P.B. Armentrout, Guided ion beam studies of the reactions of Ti^+, V^+, and Cr^+ with silane. Electronic state effects, comparison to reactions with methane, and M^+–SiH_x (x = 0–3) bond energies, J. Am. Chem. Soc. 116 (1994) 10742–10750.
[39] B.L. Kickel, P.B. Armentrout, Guided ion beam studies of the reactions of Mn^+, Cu^+, and Zn^+ with silane. M^+–SiH_x (x = 0–3) bond energies, J. Phys. Chem-US 99 (1995) 2024–2032.

[40] B.L. Kickel, P.B. Armentrout, Reactions of Fe^+, Co^+, and Ni^+ with silane. Electronic state effects, comparison to reactions with methane, and M^+–SiH_x (x = 0–3) bond energies, J. Am. Chem. Soc. 117 (1995) 764–773.
[41] G.R. Gillson, D.J. Douglas, J.E. Fulford, K.W. Halligan, S.D. Tanner, Nonspectroscopic interelement interferences in inductively coupled plasma mass spectrometry, Anal. Chem. 60 (1988) 1472–1474.
[42] D.J. Douglas, personal, communication, (1996, 2011).
[43] A.L. Gray, Communication. Influence of load coil geometry on oxide and doubly charged ion response in inductively coupled plasma source mass spectrometry, J. Anal. At. Spectrom. 1 (1986) 247–249.
[44] K.I. Sakata, K. Kawabata, Reduction of fundamental polyatomic ions in inductively coupled plasma mass spectrometry, Spectrochim. Acta Part B 49 (1994) 1027–1038.
[45] N.S. Nonose, N. Matsuda, N. Fudagawa, M. Kubota, Some characteristics of polyatomic ion spectra in inductively coupled plasma mass spectrometry, Spectrochim. Acta Part B 49 (1994) 955–974.
[46] H.B. Lim, R.S. Houk, J.S. Crain, Langmuir probe measurements of potential inside a supersonic jet extracted from an inductively coupled plasma, Spectrochim. Acta Part B 44 (1989) 989–998.
[47] B.B. Schneider, D.D.Y. Chen, Collision-induced dissociation of ions with the orifice-skimmer region of an electrospray mass spectrometer, Anal. Chem. 72 (2000) 791–799.
[48] S.M. McIntyre, J.W. Ferguson, R.S. Houk, Determination of dissociation temperature for ArO^+ in inductively coupled plasma-mass spectrometry: effects of excited electronic states and dissociation pathways, Spectrochim. Acta Part B 66 (2011) 581–587.
[49] J.E. Patterson, B.S. Duersch, P.B. Farnsworth, Optically determined velocity distributions of metastable argon in the second stage of an inductively coupled plasma mass spectrometer, Spectrochim. Acta Part B 54 (1999) 537–544.
[50] W.N. Radicic, J.B. Olsen, R.V. Nielson, J.H. Macedone, P.B. Farnsworth, Characterization of the supersonic expansion in the vacuum interface of an inductively coupled plasma mass spectrometer by high-resolution diode laser spectroscopy, Spectrochim. Acta Part B 61 (2006) 686–695.
[51] N. Taylor, P.B. Farnsworth, Experimental characterization of the effect of skimmer cone design on shock formation and ion transmission efficiency in the vacuum interface of an inductively coupled plasma mass spectrometer, Spectrochim. Acta Part B (2012) submitted for publication.